Larmor time of a wave packet tunneling through a barrier with an infinitesimal magnetic field

Duo Wang and Libin Fu*

Graduate School, China Academy of Engineering Physics, Beijing 100193, China

(Received 4 September 2024; revised 13 July 2025; accepted 19 September 2025; published 14 October 2025)

Recently, experimental measurements of the Larmor time of incident wave packets have been conducted, once again drawing attention to such a time. These experiments measured the tunneling time of Bose-condensed ^{87}Rb atoms, with theoretical analyses employing free particles. In this paper, we investigate the tunneling process of wave packets, which, unlike free particles with a definite incident energy, have a continuous distribution of energies. We show how the Larmor time $\tau_{z(y)}$ for a wave packet tunneling through a barrier depends on the barrier width d, the barrier's characteristic wave vector k_0, the incident wave packet's central wave vector k_c, and its width σ in wave-number space. When the barrier width d is small, we find that $\tau_{z(y)}$ varies monotonically. For wide barriers ($d > 2.0\pi$), we find an anomaly where wave packets with lower incident energy or higher barriers have shorter tunneling times, which is consistent with recent experimental results. Additionally, for narrow wave packets in wave-number space ($\sigma < \gamma$), where γ is the width of the fitted Fano peak, the results are generally consistent with those for plane waves. However, as the wave packet widens in wave-number space, the maximum points of $\tau_{z(y)}$ will undergo a nonlinear decrease and σ significantly affects the maximum Larmor time.

DOI: 10.1103/bm9q-r6j9

I. INTRODUCTION

Quantum tunneling is one of the most distinctive phenomena in quantum mechanics. The question of how long a particle spends in the barrier region is not a new one. It has troubled us for nearly a century [1], but remains far from being resolved, primarily because time is a parameter rather than a quantum operator [2]. Ongoing debates have generated a significant amount of literature [3–8]. The efforts to define, to understand, to measure, and to interpret the value of tunneling time have been ongoing, achieved through examining the scattering process of incident waves hitting the barrier. The early well-known research on tunneling time was conducted by Eisenbud [9], Bohm [10], and Wigner [11], known as the "phase time." Moreover, Smith [12] introduced the dwell time, which was initially introduced and defined by Büttiker [13] in the one-dimensional case. Additionally, there are traversal times initially reported by Büttiker and Landauer [14], as well as the complex time proposed by Sokolovski and Baskin [15] as a formal generalization of the classical time concept to the quantum domain and so forth. Among them, Larmor time [13,16–19] is measured using the Larmor precession as a clock [20], in the case of an infinitesimal field.

The discussion of the Larmor time can indeed be traced back to as early as 1966, when Baz [21] proposed a thought experiment to measure the time spent in the barrier region using a Larmor clock. Subsequently, Rybachenko [22] used Baz's idea in the one-dimensional case. The pioneers studied the effects on the spin components in a plane orthogonal to the field. However, it is not just the components in the plane that are affected; the spin component parallel to the field is also influenced. Consequently, this led Büttiker to introduce the "Larmor time" [13], based on the spin component parallel to the field. All the considerations above relate to the Larmor time of plane-wave incidence. Later, it was demonstrated that the spin precession time and the dwell time of neutral spinning particles in a one-dimensional rectangular potential well [23] and barrier [24] are equal. Additionally, the Larmor time of a bound electron wave packet tunneling through a barrier has been calculated recently [25]. On the experimental side, early measurements of the Larmor time have been conducted in optical systems [26,27] and neutrons [28]. Notably, recent experimental measurements of the Larmor time of tunneling atoms, regarded as wave packets, have been conducted [16–18]. In these experiments, the time it takes for ^{87}Rb atoms to tunnel through an optical barrier was measured and further investigation was conducted on the influence of incident energy on tunneling time. However, there has always been a lack of theoretical analysis concerning the impact of wave-packet parameters, such as the central wave vector and width in wave-number space, on the Larmor time.

In this paper, we investigate the spin change of the wave packet after tunneling is completed, especially in the small field. It is important to note that we are not considering arbitrary wave packets, but rather incoming wave packets that meet certain conditions: the incoming wave packet is initially far from the barrier and the distribution of momentum is almost negligible for negative values. Therefore, the initial wave packet only has a forward component, which greatly simplifies the calculations. Subsequently, by applying the small-field approximation and defining the structure factors in the y and z directions, we ultimately derive the integral representation of the Larmor time $\tau_{z(y)}$ for the tunneling of a wave packet. We find that the Larmor time of the wave-packet tunneling depends strongly not only on the parameters of the

*Contact author: lbfu@gscaep.ac.cn

wave packet, such as its width in wave-number space and central wave vector, but also on the barrier height and width. This is actually the result of the competition between two parameters: the width of the wave packet in wave-number space and the width of the structure factor $f^{z(y)}$, which is defined in Sec. IV. Additionally, when the width of the wave packet in wave-number space is small, its tunneling results are consistent with those of plane waves, which is in agreement with the numerical simulation results of the time evolution of the Gaussian wave packet [29].

II. LARMOR TUNNELING TIME OF INCIDENT PLANE WAVES

In the study of tunneling of incident plane waves through potential barriers, we consider particles with mass m and kinetic energy E, which can be represented by the wave vector k such that $E = \hbar^2k^2/2m$, interacting with a rectangular barrier of height V_0 and width d. The particles move along the y direction with the barrier centered at $y = 0$ and, in this context, the transmitted wave can be expressed as De^{iky}. It is well known that [30] the amplitude of the transmitted wave can be written as $D = T^{1/2}e^{i\Delta\phi}e^{-ikd}$, where

$$T = \left[1 + \frac{(k^2+\kappa^2)^2}{4k^2\kappa^2}\sinh^2(\kappa d)\right]^{-1} \tag{1}$$

is the transmission probability and the phase increase across the barrier, $\Delta\phi$, satisfies $\tan(\Delta\phi) = \frac{k^2-\kappa^2}{2\kappa k}\tanh(\kappa d)$. Here, we similarly use the barrier's characteristic wave vector k_0 to represent $V_0 = \hbar^2k_0^2/2m$. Consequently, we have $\kappa = \sqrt{2m(V_0-E)}/\hbar = \sqrt{k_0^2-k^2}$ for energies $E < V_0$.

However, the study of Larmor times for incident plane waves relies on a weak magnetic field localized within the barrier region, oriented along the z axis, and represented as $\mathbf{B_0} = B_0\hat{z}$. When particles with spin $s = \frac{1}{2}$ are in the magnetic-field region, they will begin Larmor precession with a frequency of $\omega_L = e|\mathbf{B_0}|/mc$, where e is the electron charge and c is the speed of light, and the component of spin parallel to the field will have a higher energy. In other words, the effect of the magnetic field $\mathbf{B_0}$ is to change the height V_0 of the barrier to $V_+ = V_0 - \hbar\omega_L/2$ ($V_- = V_0 + \hbar\omega_L/2$) for the spin-up (spin-down) component. Thus, the total Hamiltonian of the system under consideration, which is also mentioned in the textbook [31], is

$$H = \begin{cases} \left(\frac{p^2}{2m} + V_0\right)\mathbb{I} - \frac{\hbar\omega_L}{2}\sigma_z, & |y| \leqslant d/2, \\ \frac{p^2}{2m}\mathbb{I}, & |y| \geqslant d/2, \end{cases} \tag{2}$$

where $\mathbb{I}$ is the unit 2×2 matrix and $\sigma_x, \sigma_y, \sigma_z$ are the Pauli spin matrices. The incident particles are polarized along the x axis, with $\psi = \frac{1}{\sqrt{2}}(1\ \ 1)^{\mathrm{T}}e^{iky}$. Since H is diagonal in the spinor basis, the spinor wave function of the transmitted particle is

$$\psi = \frac{1}{\sqrt{|D_+|^2 + |D_-|^2}}\begin{pmatrix} D_+ \\ D_- \end{pmatrix}, \tag{3}$$

where D_+ and D_- are the amplitudes of the transmitted wave with κ replaced by $\kappa_\pm = \sqrt{2m(V_\pm - E)}/\hbar$, respectively. This transmitted spinor wave function reveals the particle's spin behavior: it not only undergoes Larmor precession in the x-y plane, but also acquires a polarization component parallel to the field while tunneling through the barrier, as expressed by

$$\langle S_z\rangle = \frac{\hbar}{2}\langle\psi|\sigma_z|\psi\rangle = \frac{\hbar}{2}\frac{T_+ - T_-}{T_+ + T_-}, \tag{4}$$

$$\langle S_y\rangle = \frac{\hbar}{2}\langle\psi|\sigma_y|\psi\rangle = -\hbar\,\sin(\Delta\phi_+ - \Delta\phi_-)\frac{(T_+T_-)^{1/2}}{T_+ + T_-}. \tag{5}$$

In the limit of an infinitesimal field, Büttiker [13] introduced the characteristic times $\tau_{y,z}$ such that $\langle S_z\rangle \triangleq (\hbar/2)\omega_L\tau_z$ and $\langle S_y\rangle \triangleq -(\hbar/2)\omega_L\tau_y$, and derived them through first-order expansion of the spin expectation value with respect to the Larmor frequency ω_L:

$$\tau_y = -(m/\hbar\kappa)\partial\Delta\phi/\partial\kappa, \tag{6}$$

$$\tau_z = -(m/\hbar\kappa)\partial\,\ln T^{1/2}/\partial\kappa. \tag{7}$$

III. LARMOR TUNNELING OF A WAVE PACKET

In this section, we consider Larmor tunneling of a wave packet and the system's Hamiltonian can still be expressed by Eq. (2). The incident particle with spin $s = \frac{1}{2}$ is polarized in the x direction and represented as $\psi(t=0) = \frac{1}{\sqrt{2}}(1\ \ 1)^{\mathrm{T}}\psi_{\mathrm{in}}(y)$ in the spinor basis, where the initial state $\psi_{\mathrm{in}}(y)$ of the particle is a Gaussian wave packet with a center at y_0, a central wave vector of k_c, and a width of σ in k space (In fact, the width of the wave packet in real space is not involved here; for simplicity, we will refer to the width of the wave packet in k space as simply the wave-packet width in the following discussions, which will not cause any confusion.), which can be expanded in the following form:

$$\psi_{\mathrm{in}}(y) = \int_{-\infty}^{\infty}\varphi(k)\left[\frac{1}{\sqrt{2\pi}}e^{iky}\right]dk, \tag{8}$$

where $\varphi(k) = \frac{1}{(2\pi\sigma^2)^{\frac{1}{4}}}e^{-iky_0}e^{-\frac{(k-k_c)^2}{4\sigma^2}}$, satisfying the following conditions:

$$\psi_{\mathrm{in}}(y \geqslant -d/2) \simeq 0, \quad \varphi(k \leqslant 0) \simeq 0, \tag{9}$$

as shown in Fig. 1. In other words, the incident wave packet is localized in the region of real space where $y < -d/2$, and in momentum space it is localized near k_c, with the distribution for $k < 0$ being negligible. Under these conditions, the expansion coefficients of the initial state in the eigenstates of backward propagation are approximately zero, while those in the eigenstates of forward propagation are approximately $\varphi(k)$. Thus, Eq. (8) can be approximated as follows:

$$\psi_{\mathrm{in}}(y) \simeq \int_0^{\infty}\varphi(k)\left(\frac{1}{\sqrt{2\pi}}\psi_k^{(+)}(y)\right)dk, \tag{10}$$

where $\psi_k^{(+)}(y)$ is the eigenstate and the corresponding eigenvalue is $E(k) = \frac{\hbar^2k^2}{2m}$ of the system under the condition of zero magnetic field ($\omega_L = 0$).

After time t, the wave function of the transmitted particle can be expanded as:

$$\psi_T^{\pm}(y,t) = \int_0^{\infty}\varphi(k)D_{\pm}(k)e^{iky}e^{-\frac{i}{\hbar}\frac{\hbar^2k^2}{2m}t}dk, \tag{11}$$

where $\pm$ corresponds to the case of potential energy $V = V_\pm$, respectively.

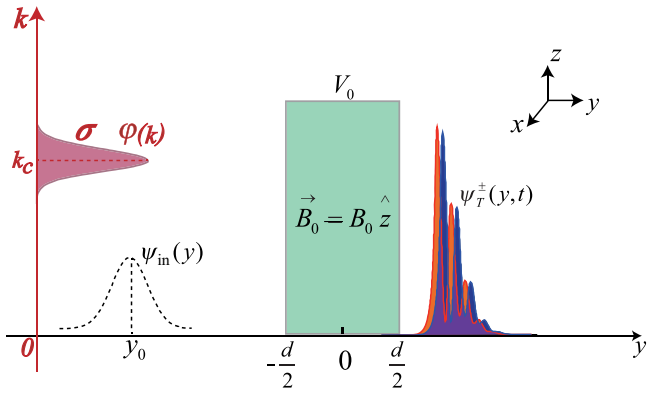

FIG. 1. Larmor clock. Sketch of wave-packet tunneling: a spin-1/2 particle is initially polarized along the x axis and tunnels through a square barrier with width d and height V_0. A magnetic field $\mathbf{B_0}$ pointing along the z axis is confined within the barrier. When the particle enters the magnetic-field region, it begins to undergo Larmor precession.

The spinor wave function of the transmitted particle is

$$\psi_T(t) = \mathcal{N}\begin{pmatrix} \int_0^\infty \varphi(k) D_+(k) e^{iky} e^{-\frac{i}{\hbar}\frac{\hbar^2 k^2}{2m}t} dk \\ \int_0^\infty \varphi(k) D_-(k) e^{iky} e^{-\frac{i}{\hbar}\frac{\hbar^2 k^2}{2m}t} dk \end{pmatrix}, \tag{12}$$

where the normalization coefficient $\mathcal{N}$ is

$$\mathcal{N} = \frac{1}{\sqrt{2\pi}} \frac{1}{\sqrt{\int_0^\infty |\varphi(k)|^2 (|D_+|^2 + |D_-|^2) dk}}. \tag{13}$$

Following an approach analogous to Büttiker's plane-wave treatment [13], we derive the expectation values

$$\begin{aligned} \langle S_z \rangle &= \frac{\hbar}{2} \langle \psi_T | \sigma_z | \psi_T \rangle \\ &= \frac{\hbar}{2} \mathcal{N}^2 \int_{-\infty}^{\infty} (|\psi_T^+(y,t)|^2 - |\psi_T^-(y,t)|^2) dy \\ &= \frac{\hbar}{2} \frac{\int_0^\infty |\varphi(k)|^2 (T_+ - T_-) dk}{\int_0^\infty |\varphi(k)|^2 (T_+ + T_-) dk}, \end{aligned} \tag{14}$$

$$\begin{aligned} \langle S_y \rangle &= \frac{\hbar}{2} \langle \psi_T | \sigma_y | \psi_T \rangle \\ &= \frac{\hbar}{2} \frac{\int_0^\infty |\varphi(k)|^2 (-2)\sqrt{T_+ T_-} \sin(\Delta\phi_+ - \Delta\phi_-) dk}{\int_0^\infty |\varphi(k)|^2 (T_+ + T_-) dk}. \end{aligned} \tag{15}$$

In the infinitesimal field, we can obtain the imbalance $T_+ - T_-$, of the transmission coefficients as $\frac{\partial T}{\partial V_0}(V_+ - V_-)$, and we obtain $T_+ + T_- \cong 2T$ and $T_+ - T_- \cong -\frac{m\omega_L}{\hbar\kappa}\frac{\partial T}{\partial \kappa}$, where we use the equation $\frac{\partial T}{\partial V_0} = \frac{\partial T}{\partial \kappa}\frac{\partial \kappa}{\partial V_0} = \frac{\partial T}{\partial \kappa}\frac{m}{\kappa\hbar^2}$. Consequently, we find that for $E < V_0$

$$\langle S_z \rangle \approx -\frac{m\omega_L}{4} \frac{\int_0^\infty |\varphi(k)|^2 T_{\kappa\kappa} dk}{\int_0^\infty |\varphi(k)|^2 T dk}, \tag{16}$$

$$\langle S_y \rangle \approx \frac{m\omega_L}{2} \frac{\int_0^\infty |\varphi(k)|^2 T \Delta\phi_{\kappa\kappa} dk}{\int_0^\infty |\varphi(k)|^2 T dk}, \tag{17}$$

where

$$\begin{aligned} T_{\kappa\kappa} &= \frac{1}{\kappa}\frac{\partial T}{\partial \kappa} \propto \frac{\partial T}{\partial V_0} \\ &= -\frac{4k_0^2 k^2 \left[2(\kappa^2 - k^2)\sinh^2(\kappa d) + k_0^2 d\kappa \sinh(2\kappa d)\right]}{\left[4k^2\kappa^2 + (k^2+\kappa^2)^2 \sinh^2(\kappa d)\right]^2}, \\ \Delta\phi_{\kappa\kappa} &= \frac{1}{\kappa}\frac{\partial \Delta\phi}{\partial \kappa} \propto \frac{\partial \Delta\phi}{\partial V_0} \\ &= -\frac{k}{\kappa}\frac{k_0^2 \sinh(2\kappa d) + 2\kappa d(\kappa^2 - k^2)}{4k^2\kappa^2 + (k^2+\kappa^2)^2 \sinh^2(\kappa d)}. \end{aligned} \tag{18}$$

For $E > V_0$, we have to replace κ by $i\mathrm{K}$, where $\mathrm{K} = \sqrt{2m(E - V_0)}/\hbar$.

In the following calculations, we respectively set the characteristic wave vector to $k_0 = \sqrt{2mV_0}/\hbar = 1$ a.u. (corresponding to $V_0 = 0.5$ a.u.) and the central wave vector to $k_c = 1$ a.u. for convenience. We check that it exhibits linear response when $B_0 = 1.2$ a.u., indicating a small field. Atomic units are used throughout the paper unless stated otherwise.

IV. LARMOR TIMES FOR TRANSMITTED PARTICLES

In the previous section, we calculated the spin expectation value for transmitted particles. Accordingly, we can derive the Larmor time $\tau_{z(y)}$ for the tunneling of a wave packet, which can be expressed as follows:

$$\tau_z \triangleq \frac{\langle S_z \rangle}{(\hbar/2)\omega_L} = \frac{1}{2}\frac{\int_0^\infty |\varphi(k)|^2 f^z dk}{\int_0^\infty |\varphi(k)|^2 T\, dk}, \tag{19}$$

$$\tau_y \triangleq \frac{\langle S_y \rangle}{-(\hbar/2)\omega_L} = \frac{\int_0^\infty |\varphi(k)|^2 f^y dk}{\int_0^\infty |\varphi(k)|^2 T\, dk}, \tag{20}$$

where the structure factors in the y and z directions are defined as $f^z \triangleq -T_{\kappa\kappa}$ and $f^y \triangleq -T\Delta\phi_{\kappa\kappa}$, respectively, and they are related to the barrier parameters (k_0, d).

From Eqs. (19) and (20), we find that when compared to plane waves, the Larmor time $\tau_{z(y)}$ for wave-packet tunneling arises from averaging the Larmor times of the constituent plane-wave components, which are proportional to the variation rate of the transmission probability T and that of the phase increase $\Delta\phi$, respectively. Furthermore, we know that the Larmor time $\tau_{z(y)}$ depends not only on the incident wave packet $\varphi(k)$, but also on the transmission probability T and the structure factor $f^{z(y)}$. Next, we will analyze these variables individually and examine how $f^{z(y)}$ significantly affects the Larmor times.

A. Structure factors $f^{z(y)}$

In our study, we first fix the barrier's characteristic wave vector at $k_0 = 1$. Consequently, the transmission probability T depends on both the barrier width d and the incident energy $E = k^2/2$. In Fig. 2, we have plotted the transmission probability T as a function of k for various barrier widths. For small barrier widths like $d = 0.1\pi$ or $d = 0.6\pi$, the transmission probability increases smoothly and monotonically. However, for larger barrier widths ($d > 2.0\pi$), the transmission probability rapidly increases from 0 to 1 near $k = k_0$ and then begins to oscillate, with 1 as its maximum value. Additionally, as

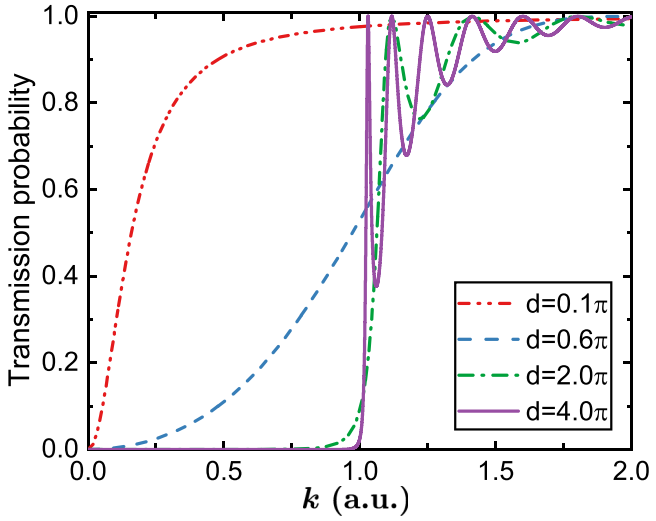

FIG. 2. Transmission probabilities for $k_0 = 1$ a.u. at barrier widths $d = 0.1\pi$, 0.6π, 2.0π, and 4.0π a.u.

the barrier width d increases, the oscillations become more pronounced.

The structure factor f^z is proportional to the partial derivative of the transmission probability T with respect to the barrier height V_0, characterizing the responsive behavior of the transmission probability. We have plotted its variation with k using black curves in Fig. 3, for various barrier widths at a fixed characteristic wave vector $k_0 = 1$. We find that, as the barrier width d increases, the structure factor f^z gradually exhibits a significantly asymmetric line shape profile. Therefore, we attempt to fit f^z using the Fano formula, which is

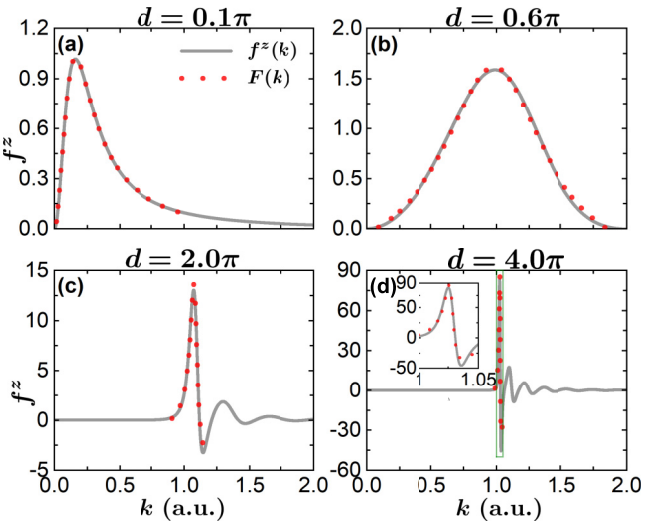

FIG. 3. Black curves represent the structure factor f^z changing with k for $k_0 = 1$ a.u., while the red lines represent the fitting curves of f^z using the Fano formula. Panels (a) to (d) correspond to barrier widths $d = 0.1\pi$, 0.6π, 2.0π, and 4.0π a.u. The inset in subfigure (d) is a magnified view of the green-boxed region.

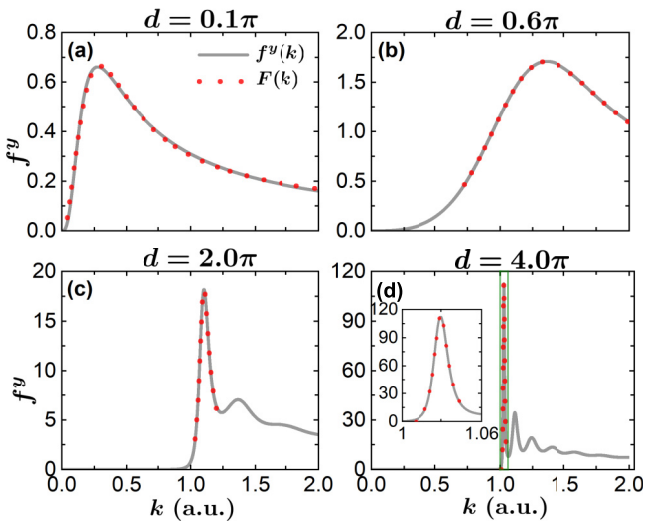

FIG. 4. Black curves represent the structure factor f^y changing with k for $k_0 = 1$ a.u., while the red lines represent the fitting curves of f^y using the Fano formula. Panels (a) to (d) correspond to barrier widths $d = 0.1\pi$, 0.6π, 2.0π, and 4.0π a.u. The inset in subfigure (d) is a magnified view of the green-boxed region.

expressed as:

$$F(k) = R\left[\frac{\left(q\frac{\gamma}{2} + k - k_{\text{res}}\right)^2}{\left(\frac{\gamma}{2}\right)^2 + (k - k_{\text{res}})^2} + a\right], \tag{21}$$

where γ represents the width of the fitted Fano peak, k_{res} represents the peak center, and the fitted curve $F(k)$ is plotted together with f^z on the same graph. Similarly, the results for f^y are shown in Fig. 4. Please note that the data range used to fit the structure factor $f^{z(y)}$ is not the entire interval (0, 2), but only the single peak region represented by the red line in the figure. This is because this peak region has the greatest influence on the Larmor time.

In Figs. 3 and 4, we observe that the red dashed line and the black solid line almost overlap in the fitting region, indicating a good fit of the Fano peak to $f^{z(y)}$. Additionally, we observe that, as the barrier width d increases, the variation range of $f^{z(y)}$ also expands, from approximately 1 at $d = 0.1\pi$ to about 100 at $d = 4.0\pi$. Regarding the shape of the structure factor $f^{z(y)}$, specifically the fitting parameters γ and k_{res} that determine its width and center, they also exhibit certain trends as d increases. To more intuitively observe how γ and k_{res} change with d, we plot the curves of k_{res} and γ as functions of d in Fig. 5.

In Fig. 5, we observe that the width γ of the Fano peak initially increases and then decreases towards zero with increasing barrier width d, while the center k_{res} of the Fano peak initially increases and gradually stabilizes around k_0. This behavior is readily understandable since k_{res} corresponds to the maximum of the structure factor $f^{z(y)}$. Recall that f^z and f^y are proportional to the variation rate of the transmission probability T and that of the phase increase $\Delta\phi$, respectively. For larger barrier widths ($d > 2.0\pi$), both T and $\Delta\phi$ undergo significant variations near k_0, resulting in the maximization of $f^{z(y)}$ in the vicinity of k_0. It can be inferred that when $d > 2.0\pi$, both γ and k_{res} remain almost unchanged.

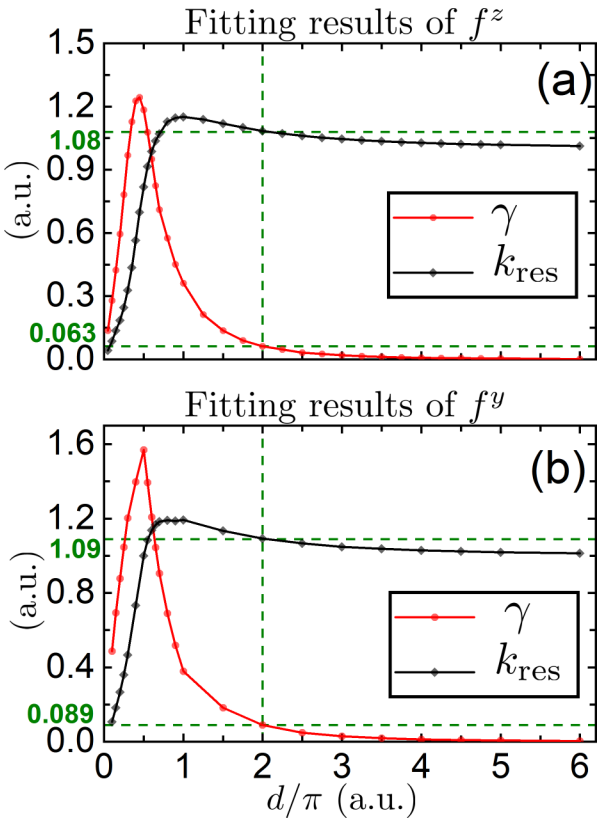

FIG. 5. Center $k_{\rm res}$ and width γ changing with the barrier width d, in units of π, for $k_0 = 1$ a.u. Panels (a) and (b) respectively show the results of fitting the structure factor f^z and f^y using Fano line shape. The green dashed lines mark the center $k_{\rm res}$ and width γ of the fitted Fano peak at $d = 2\pi$ a.u.

B. Larmor times

From the previous analysis with the fixed characteristic wave vector $k_0 = 1$, we know that the Larmor time $\tau_{z(y)}$ for a wave packet tunneling through a barrier is sensitively dependent on the barrier width d and the parameters k_c and σ of the incident wave packet. Figure 6 presents the contour map of the Larmor time $\tau_{z(y)}$ as a function of the wave-packet parameters $(k_c/k_0,\ \sigma)$ for different barrier widths d. When the barrier width d is small, we find that $\tau_{z(y)}$ varies monotonically, as shown in Figs. 6(a) and 6(d). From the previous analysis, it is evident that when the barrier width $d < 2.0\pi$, both the center $k_{\rm res}$ and the width γ vary sensitively with changes in the barrier width d, unlike when $d > 2.0\pi$, where they remain almost constant. Furthermore, the range of $f^{z(y)}$ is comparable to that of the transmission probability T in the denominator of Eqs. (19) and (20), implying that their coupled influence on the Larmor time $\tau_{z(y)}$ must be considered jointly. Overall, while the analysis of Larmor time $\tau_{z(y)}$ for narrow barriers is relatively complex, it is noteworthy that the variation in Larmor time $\tau_{z(y)}$ ultimately follows a simple trend, changing monotonically with the wave-packet parameters k_c and σ.

As the barrier width d increases (e.g., $d = 2.0\pi$), we find that $\tau_{z(y)}$ does not vary monotonically with the parameters k_c and σ. For particularly narrow wave packets (e.g., $\sigma = 0.01$), the Larmor time for a wave packet tunneling through a barrier closely matches that of a plane wave, as seen in Fig. 7. This result is expected. When the wave packet is very narrow in k space, its momentum distribution becomes highly localized around the central wave vector k_c, resulting in quantum tunneling behavior nearly indistinguishable from a plane wave characterized by wave vector k_c and energy $E = \hbar^2 k_c^2/2m$.

From Figs. 6(b) and 6(e), as σ increases, $\tau_{z(y)}$ initially increases and then decreases. Furthermore, for a given width of the incident wave packet, we find that $\tau_{z(y)}$ initially increases monotonically with k_c, indicating that lower incident energy leads to faster tunneling, and then gradually decreases. This behavior is well known, as shown in Fig. 7(b), where the Larmor time $\tau_{z(y)}$ for plane-wave tunneling also follows this trend. Moreover, for wave packets, the transition point of this trend, the incident central wave vector k_c corresponding to maximum Larmor time, can be characterized by the center $k_{\rm res}$ of the Fano peak. Specifically, when the wave-packet width σ is less than the Fano peak width γ ($\sigma < \gamma$), the maximum Larmor time $\tau_{z(y)}$ approximately occurs at $k_c = k_{\rm res}$ (a result that evidently holds for plane waves as well). Figure 7(b) clearly illustrates this result, showing cases of both plane-wave incidence and wave-packet incidence with widths ($\sigma = 0.01 < \gamma = 0.063, 0.089$). Indeed, when $d > 2.0\pi$, the range of Fano peaks extends beyond the range of transmission probability T, which typically ranges from 0 to 1. Therefore, we should first consider the influence of $f^{z(y)}$ in the numerator of Eqs. (19) and (20). When k_c approaches $k_{\rm res}$, this ensures that the overlap between the initial wave-packet distribution $|\varphi(k)|^2$ and the $f^{z(y)}$ is maximized, thereby guaranteeing that the integrals in the numerator of Eqs. (19) and (20) are maximized.

Due to the variable sign of f^z, which is not always positive, as shown in Figs. 3(c) and 3(d), the transition point k_c of τ_z should decrease as σ increases, to ensure that the integral term of the numerator is not excessively canceled out by positive and negative contributions. The transition point k_c of τ_y follows a similar changing pattern because the transmission probability T is nearly zero for $k < 1$. Decreasing k_c in this case can make the denominator nearly zero, thereby allowing τ_y to achieve a maximum. In Figs. 6(b) and 6(e), we can clearly see that, on the left side of $\sigma = \gamma$, the transition point k_c of $\tau_{z(y)}$ approximately occurs near $k_{\rm res}$, whereas, on the right side of $\sigma = \gamma$, the transition point k_c of $\tau_{z(y)}$ decreases gradually with increasing σ.

As the barrier width increases from $d = 2.0\pi$ to $d = 4.0\pi$, we observe a leftward shift in the green lines marking the width γ of $f^{z(y)}$, accounting for the differences between panels (b) and (c), (e) and (f) in Fig. 6. What is remarkable is that for wide barriers [as shown in Figs. 6(b) and 6(c)], such as $d = 2.0\pi$ and 4.0π, the Larmor time τ_z exhibits negative values. The fundamental reason for the occurrence of negative Larmor times is that, as the barrier width increases, the transmission probability oscillates sharply with incident energy, while, for narrow barriers, the transmission probability increases monotonically. For particles entering the barrier region, their wave-number components will be described by different wave numbers $k_\pm = \sqrt{k^2 \pm \frac{m\omega_L}{\hbar}}$. Due to the sharp oscillations in the transmission probability, a measurable range may occur where the

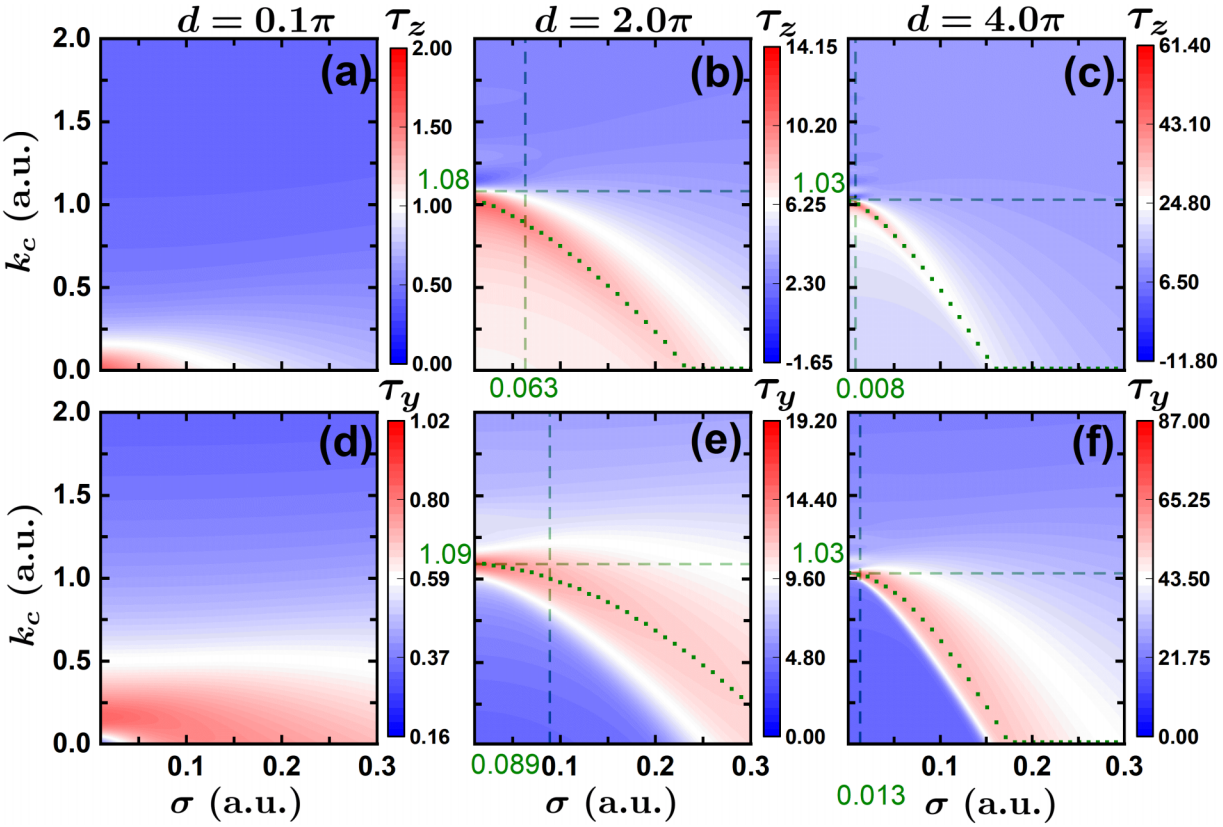

FIG. 6. Panels (a) to (c) are Larmor times $\tau_z(k_c/k_0, \sigma)$ for $d = 0.1\pi$, 2.0π, and 4.0π a.u. at $k_0 = 1$ a.u., and (d) to (f) are Larmor times τ_y. The green lines (vertical and horizontal) represent the width γ and center k_{res} of $f^{z(y)}$, respectively. The maximum points of $\tau_{z(y)}$ in the $\frac{k_c}{k_0}$-σ plane are mapped by the green dashed curves.

transmission probability decreases, i.e., $T(k_+) - T(k_-) < 0$, which leads to the appearance of negative peaks in the structure factor f^z and negative regions in the Larmor time τ_z. Therefore, the existence of negative Larmor times could reflect the trend of variation in the transmission probability for different barrier widths.

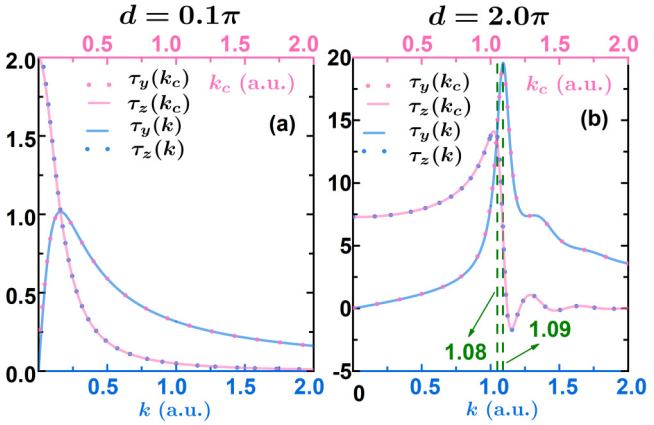

FIG. 7. Blue lines (solid, dashed) represent the Larmor times (τ_y, τ_z) for plane waves with incident energy $E = \hbar^2 k^2/2m$, with $k_0 = 1$ a.u., whereas the red lines (dashed, solid) represent the Larmor times (τ_y, τ_z) for wave packets centered at k_c with a width of $\sigma = 0.01$ a.u. The position of the center k_{res} is marked by the green lines in panel (b).

All the conclusions presented above concerning the Larmor time were obtained with $k_0 = 1$ while varying the central wave vector k_c of the wave packet from 0 to 2. However, the constraints prescribed by Eq. (9) for incident wave packets make the region with small k_c computationally inaccessible due to large errors. To address this challenge, we fixed $k_c = 1$ and increased k_0, effectively exploring the low-incident-energy region ($k_c/k_0 < 0.5$), with the corresponding results shown in Fig. 8. This figure reveals that, in the low-incident-energy region, the maximum Larmor time exhibits significantly different behavior compared to the previously discussed case with fixed k_0, motivating our focus on it in subsequent discussion.

C. Maximum Larmor time

In Fig. 8, similarly, we observe that, as the barrier width increases (e.g., $d = 2.0\pi$), the Larmor time $\tau_{z(y)}$ no longer changes monotonically with the barrier's characteristic wave vector k_0. Instead, it first increases and then decreases as k_0 increases. It is easy to see that the recent experimental conclusions [18] are consistent with the results in the regions below the green dashed curves in Figs. 6 and 8, suggesting that the wave packets used in the experiment are not too wide.

We have plotted the curves drawn from the maximum points $(\sigma, \frac{1}{k_0})$ of the Larmor time $\tau_{z(y)}$ in Fig. 9 for different barrier widths at a fixed central wave vector $k_c = 1$ a.u. We find that these curves exhibit a typical "gradual transition"

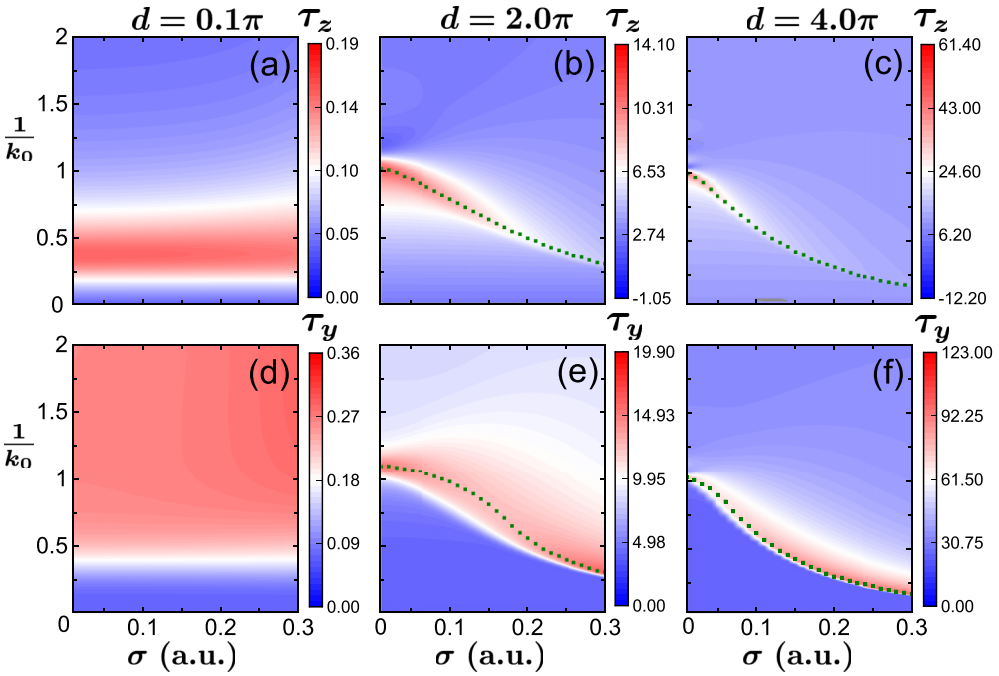

FIG. 8. Panels (a) to (c) are Larmor times $\tau_z(k_c/k_0, \sigma)$ for $d = 0.1\pi$, 2.0π, and 4.0π a.u. at $k_c = 1$ a.u., and (d) to (f) are Larmor times τ_y. The maximum points of $\tau_{z(y)}$ in the $\frac{k_c}{k_0}$-σ plane are mapped by the green dashed curves.

behavior; therefore, we attempt to fit them using the logistic function, which is expressed as:

$$L(\sigma) = \frac{A_1 - A_2}{1 + (\sigma/\sigma_0)^p} + A_2, \tag{22}$$

where A_1 and A_2 represent the boundary values of the logistic curves, σ_0 is the characteristic point where $L(\sigma_0) = \frac{A_1+A_2}{2}$, p (ranging from 1.5 to 4.5) controls the steepness of the transition from A_1 to A_2, and the fitted curves $L(\sigma)$ are also plotted on the same graph, with an excellent fitting quality characterized by the coefficient of determination $R^2 \geqslant 0.996$. Notably, Eq. (22) describes a nonlinear decrease behavior,

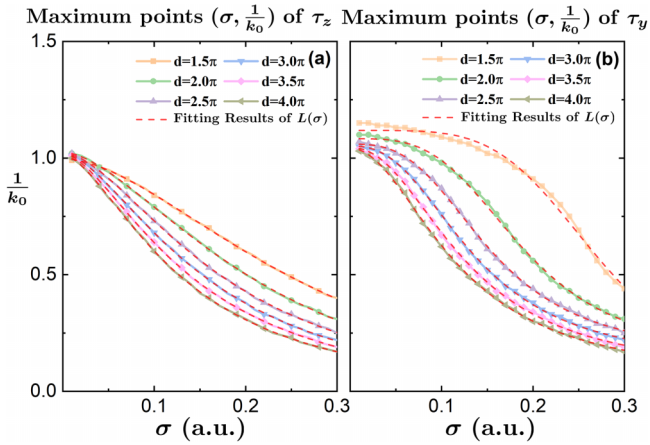

FIG. 9. Maximum points $(\sigma, \frac{1}{k_0})$ of the Larmor time $\tau_{z(y)}$ for $k_c = 1$ a.u. with barrier widths $d = 1.5\pi$, 2.0π, 2.5π, 3.0π, 3.5π, and 4.0π a.u. The red dashed line represents the fitting results using the logistic function.

where the rate of change undergoes a significant shift at the characteristic point σ_0, ultimately tending toward a steady state. According to Table I, the position of the characteristic points σ_0 shifts to smaller values with the increase in the barrier widths, suggesting that the decrease behavior described by the curves in Fig. 9 begins to accelerate.

Furthermore, in Fig. 8, when $d > 2\pi$ a.u., there exists a maximum Larmor time $\tau_{z(y)}^{\max}$ for each given wave packet width σ, and its variation with σ is plotted in Fig. 10, with mapping formula $(y - y_{\min})/(y_{\max} - y_{\min})$. In Fig. 10, we observe that $\tau_{z(y)}^{\max}$ increases monotonically with barrier width d, which is as expected. As the wave-packet width σ increases, $\tau_z^{\max}$ decreases monotonically, while $\tau_y^{\max}$ exhibits a nonmonotonic trend (decreasing then increasing), which is a rather surprising behavior. In the inset of Fig. 10(b), the zero points of the six curves, ordered from smallest to largest, correspond to barrier widths of $d = 4.0\pi$, 3.5π, 3.0π, 2.5π, 2.0π, and 1.5π a.u., respectively, suggesting that the larger the barrier width, the earlier $\tau_y^{\max}$ reaches its minimum. Thus, to reduce the tunneling time in experiments, we can choose to increase the wave-packet width σ appropriately to lower $\tau_{z(y)}^{\max}$. For τ_y, the choice of σ is related to the barrier width d. In any case,

TABLE I. Characteristic point σ_0 for barrier widths $d = 1.5\pi$, 2.0π, 2.5π, 3.0π, 3.5π, and 4.0π a.u., fitted using the logistic function $L(\sigma)$ to the maximum points $(\sigma, \frac{1}{k_0})$ of the Larmor time $\tau_{z(y)}$. The upper and lower rows correspond to the cases of τ_z and τ_y, respectively.

d/π (a.u.)	1.5	2.0	2.5	3.0	3.5	4.0
$\tau_z : \sigma_0$	0.289	0.230	0.182	0.161	0.144	0.132
$\tau_y : \sigma_0$	0.270	0.189	0.154	0.136	0.126	0.118

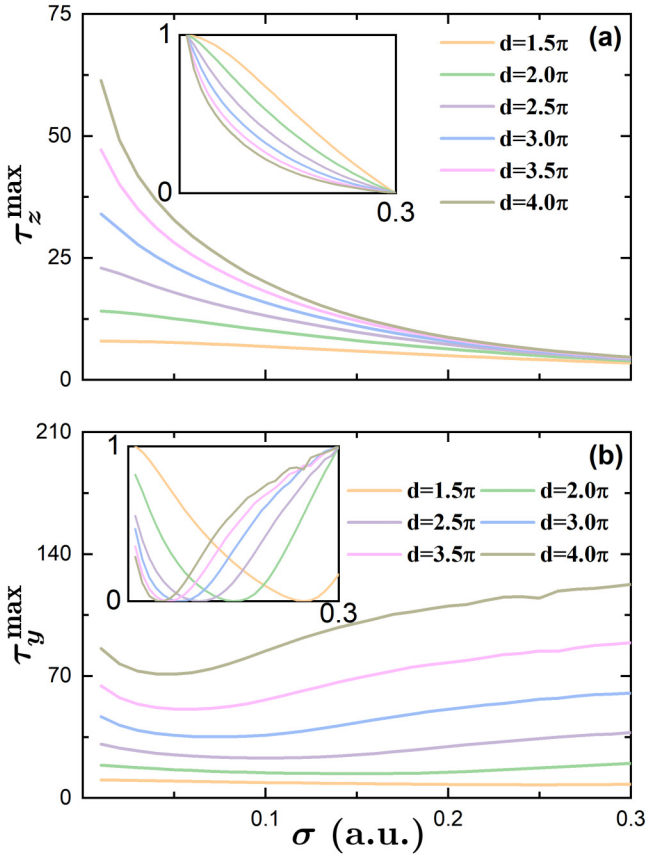

FIG. 10. (a) Maximum Larmor time $\tau_z^{\max}$ with respect to wave-packet width σ, for $k_c = 1$ a.u. and barrier widths $d = 1.5\pi$, 2.0π, 2.5π, 3.0π, 3.5π, and 4.0π a.u. (b) Corresponding results for $\tau_y^{\max}$. The insets show normalized results of mapping them to the range (0, 1).

these adjustments can be made to reduce the upper bound of tunneling time $\tau_{z(y)}$, as shown in the results of Fig. 10.

V. SUMMARY AND DISCUSSION

In summary, under the condition of infinitesimal fields, we studied the tunneling times of Gaussian wave packets and compared them with the results of plane waves. When the width σ of the incident Gaussian wave packet approaches zero, the Larmor time for tunneling through the barrier is essentially the same as that for plane waves. However, as σ increases, we need to consider the unique effects of the wave packet, which can be analyzed by the structure factor $f^{z(y)}$, and we determined its width γ by fitting it with a Fano peak. When $\sigma < \gamma$, the incident wave packet can be considered narrow; otherwise, it is wide. From this, we found that the transition points k_c of Larmor time $\tau_{z(y)}$ for narrow wave packets are determined by the center k_{res} of the Fano peak and, as the wave packet widens, the transition points k_c decrease.

The above shows the variation of Larmor time $\tau_{z(y)}$ when the barrier's characteristic wave vector k_0 is kept constant while changing the wave-packet parameters. When the central wave vector k_c is kept constant and k_0 is varied, the Larmor time $\tau_{z(y)}$ exhibits a surprising behavior in the low-incident-energy region. Further calculations reveal that the maximum points $(\sigma, \frac{1}{k_0})$ of $\tau_{z(y)}$ can be fitted by a logistic function, which describes a nonlinear decrease behavior. Additionally, the analysis of $\tau_{z(y)}^{\max}$ shows that it can be used to reduce the tunneling time in experiments.

ACKNOWLEDGMENTS

We acknowledge Dr. L. Jia from Central South University for her valuable suggestions. This work was supported by the National Natural Science Foundation of China (Grants No. 12088101 and No. U2330401).

DATA AVAILABILITY

The data that support the findings of this article are not publicly available. The data are available from the authors upon reasonable request.

[1] L. A. MacColl, Note on the transmission and reflection of wave packets by potential barriers, Phys. Rev. **40**, 621 (1932).
[2] J. G. Muga, R. S. Mayato, and I. L. Egusquiza, *Time in Quantum Mechanics*, Lecture Notes in Physics (Springer, Berlin, 2008).
[3] C. de Carvalho and H. Nussenzveig, Time delay, Phys. Rep. **364**, 83 (2002).
[4] H. G. Winful, Tunneling time, the Hartman effect, and superluminality: A proposed resolution of an old paradox, Phys. Rep. **436**, 1 (2006).
[5] E. H. Hauge and J. A. Støvneng, Tunneling times: A critical review, Rev. Mod. Phys. **61**, 917 (1989).
[6] R. Landauer and T. Martin, Barrier interaction time in tunneling, Rev. Mod. Phys. **66**, 217 (1994).
[7] S.-C. Li, A general scenario of tunneling time in different energy regimes, New J. Phys. **24**, 083033 (2022).
[8] D. Sokolovski and E. Akhmatskaya, Tunnelling times, Larmor clock, and the elephant in the room, Sci. Rep. **11**, 10040 (2021).
[9] L. Eisenbud, The formal properties of nuclear collisions, Ph.D. thesis, Princeton University, Princeton, NJ, 1948.
[10] D. Bohm, *Quantum Theory* (Prentice-Hall, Englewood Cliffs, NJ, 1951).
[11] E. P. Wigner, Lower limit for the energy derivative of the scattering phase shift, Phys. Rev. **98**, 145 (1955).
[12] F. T. Smith, Lifetime matrix in collision theory, Phys. Rev. **118**, 349 (1960).
[13] M. Büttiker, Larmor precession and the traversal time for tunneling, Phys. Rev. B **27**, 6178 (1983).
[14] M. Büttiker and R. Landauer, Traversal time for tunneling, Phys. Rev. Lett. **49**, 1739 (1982).
[15] D. Sokolovski and L. M. Baskin, Traversal time in quantum scattering, Phys. Rev. A **36**, 4604 (1987).
[16] R. Ramos, D. Spierings, I. Racicot, and A. Steinberg, Measurement of the time spent by a tunneling atom within the barrier region, Nature (London) **583**, 529 (2020).

[17] D. C. Spierings and A. M. Steinberg, Measuring the time tunneling particles spend in the barrier, in *Optical, Opto-Atomic, and Entanglement-Enhanced Precision Metrology II*, edited by S. M. Shahriar and J. Scheuer, International Society for Optics and Photonics Vol. 11296 (SPIE, Bellingham, WA, 2020), p. 112960F.

[18] D. C. Spierings and A. M. Steinberg, Observation of the decrease of Larmor tunneling times with lower incident energy, Phys. Rev. Lett. **127**, 133001 (2021).

[19] J. P. Falck and E. H. Hauge, Larmor clock reexamined, Phys. Rev. B **38**, 3287 (1988).

[20] F. Suzuki and W. G. Unruh, Numerical quantum clock simulations for measuring tunneling times, Phys. Rev. A **107**, 042216 (2023).

[21] A. I. Baz', Sov. J. Nucl. Phys. **4**, 182 (1966).

[22] V. F. Rybachenko, Time of penetration of a particle through a potential barrier, Sov. J. Nucl. Phys. **5**, 895 (1967).

[23] Z.-J. Li, Y.-H. Nie, J.-J. Liang, and J.-Q. Liang, Larmor precession and dwell time of a relativistic particle scattered by a rectangular quantum well, J. Phys. A: Math. Gen. **36**, 6563 (2003).

[24] Z.-J. Li, J. Q. Liang, and D. H. Kobe, Larmor precession and barrier tunneling time of a neutral spinning particle, Phys. Rev. A **64**, 042112 (2001).

[25] L. Jia, H. Xing, and L. Fu, Larmor time of a bound electron wave packet tunneling through a barrier, Phys. Rev. A **105**, 062804 (2022).

[26] M. Deutsch and J. E. Golub, Optical Larmor clock: Measurement of the photonic tunneling time, Phys. Rev. A **53**, 434 (1996).

[27] P. Balcou and L. Dutriaux, Dual optical tunneling times in frustrated total internal reflection, Phys. Rev. Lett. **78**, 851 (1997).

[28] M. Hino, N. Achiwa, S. Tasaki, T. Ebisawa, T. Kawai, T. Akiyoshi, and D. Yamazaki, Measurement of Larmor precession angles of tunneling neutrons, Phys. Rev. A **59**, 2261 (1999).

[29] H. M. Krenzlin, J. Budczies, and K. W. Kehr, Larmor clock for tunneling times, Phys. Rev. A **53**, 3749 (1996).

[30] C. Cohen-Tannoudji, B. Diu, and F. Laloë, *Quantum Mechanics* (Wiley, New York, 1977), p. 991.

[31] M. Razavy, *Quantum Theory of Tunneling*, 2nd ed. (World Scientific Publishing Company, Singapore, 2013).